Chromatic dispersion and losses of microstructured optical fibers

Boris Kuhlmey, Gilles Renversez, and Daniel Maystre

Using a rigorous and vector multipole method, we compute both losses and dispersion properties of microstructured optical fibers with finite cross sections. We restrict our study to triangular lattices of air-hole inclusions in a silica matrix, taking into account material dispersion. The fiber core is modeled by a missing inclusion. The influence of pitch, hole diameter, and number of hole rings on chromatic dispersion is described, and physical insights are given to explain the behavior observed. It is shown that flattened dispersion curves obtained for certain microstructured fiber configurations are unsuitable for applications because of the fibers' high losses and that they cannot be improved by a simple increase of the number of air-hole rings. © 2003 Optical Society of America

OCIS codes: 060.2270, 060.2280, 060.2400, 060.2430.

1. Introduction and Background

Microstructured optical fibers (MOFs) are generally made from regular lattices of cylindrical inclusions, for example, air holes, in a dielectric matrix. MOF cores usually consist of a defect of the lattice, which can be an inclusion of a different type or size or, in bulk core MOFs, a missing inclusion. In recent publications,[1,2] attention was drawn to the peculiar and interesting dispersion properties that MOFs can exhibit and that indicate that MOFs may be good candidates for dispersion management in optical communication systems. In this paper we use a fully vector and rigorous multipole method[3,4] that was recently developed by the present authors and by Mc Phedran and Botten[5] in Sydney to explore the dependence of chromatic dispersion on wavelength and MOF geometry. We concentrate here on a silica bulk core MOF with a triangular lattice of air holes (see Fig. 1). The most important point in which the research reported here contrasts with that on MOF dispersion published previously is that the multipole method described herein is able to deal with finite cross-section MOFs. We could therefore study the influence of the extent of the confining air-hole region on dispersion and on its associated losses.

Our multipole method is a standard multipole method extended to conical mounts. It is based on local expansions of the vector fields in Fourier Bessel series and uses addition theorems to link these local expansions. Boundary conditions are implemented analytically for circular inclusions, so the only approximations are the truncation of the Fourier Bessel series (see Refs. 4 and 6 for a complete study) as well as the fundamental hypothesis of the invariance of the fiber along its axis. If the inclusions overlap, our method is not appropriate. With the MOF geometry and the wavelength as inputs, the method gives the modes of the MOF as an output. Material dispersion can thus be included in a natural way in the MOF geometry, for example by use of Sellmeier expansions.[7,8]

A mode of a MOF is characterized by its field pattern and propagation constant β (or, equivalently, by its effective index $n_{\text{eff}} = \beta/k_0$, where k_0 is the free-space wave number). Because of the losses that result from the finite transverse extent of the confining structure, the effective index is a complex value; its imaginary part $\Im(n_{\text{eff}})$ is related to the losses $\mathscr{L}$ in decibels per meter through the relation

$$\mathscr{L} = \frac{20}{\ln(10)} \frac{2\pi}{\lambda} \Im(n_{\text{eff}}) \times 10^6 \,, \tag{1}$$
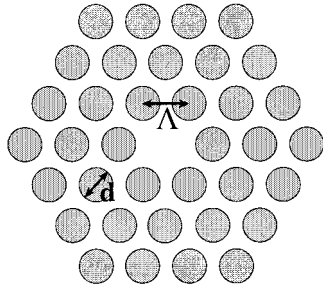
Fig. 1. Cross section of the model MOF with three rings of holes (the holes are shown colored gray); $N_r = 3$. Λ is the pitch of the triangular lattice, and d is a holes diameter. The solid core consists of one missing hole in the center of the structure.

where λ is given in micrometers. Dispersion parameter D is computed through the usual formula from the real part of effective index $\Re(n_{eff})$ (Ref. 8):

$$D = -\frac{\lambda}{c}\frac{\partial^2 \Re(n_{eff})}{\partial \lambda^2}. \qquad (2)$$

As in ordinary waveguides, the dispersion of guided modes results from both material and waveguide dispersion. The remarkable feature of MOFs is that the waveguide dispersion can be modified significantly by means of a wide range of geometrical parameters, namely, the positions and sizes of the different holes. The behavior of waveguide dispersion can be understood from heuristic considerations of effective media: At short wavelengths, light can distinguish the details of the structure, resulting in a greater concentration in the high-index region (i.e., the core whose index is that of the matrix). In this situation the effective index is smaller than the refractive index of the matrix. At longer wavelengths the structure tends to a homogeneous one, and the effective index of the mode will consequently be upper-bounded by the homogenized refractive index of the structure, which is much lower than the refractive index of the matrix as a result of the air inclusions. These heuristic considerations are unable to predict MOF chromatic dispersion precisely: A precise numerical study is required. Moreover, in practical applications the losses have a vital importance.

Detailed studies of losses in MOFs versus pitch of the air-hole lattice, the hole diameter, and the hole ring number have already been carried out by the multipole method.[4,9] A vector method that uses periodic boundary conditions[10] has already been used to study dispersion in MOFs,[11] but in this model the influence of the number of hole rings cannot be investigated, and, above all, the losses cannot be computed.

2. Validation

The method has been checked thoroughly by comparison with other numerical methods, namely; a fictitious source[12] and other multipole methods[13,14] (more details of these comparisons can be found in an earlier paper by the present authors and others.[4]

The symmetry properties of fibers are accurately satisfied[6]: For a MOF with a rotational symmetry of order 6, the fundamental mode is twofold degenerate, as expected from Mc Isaac's theory.[15]

The method that we codeveloped and its numerical implementation have also been compared with a plane-wave method for a microstructured optical fiber with a ring of six air holes of diameter $d = 5$ μm with pitch $\Lambda = 6.75$ μm and a fixed background index $n = 1.45$ at $\lambda = 1.55$ μm; the computed value $\Re(n_{eff})$ of the fundamental mode is 1.4447672.[6]

With respect to chromatic dispersion, our results are in good agreement (see Table 1) both with the dispersion and with its slope as measured by Gander and his colleagues and with the dispersion calculated by the same authors,[16] who used an expansion of the fields in terms of Hermite–Gaussian functions[1] for a microstructured optical fiber ($d = 0.621$ μm, with a pitch $\Lambda = 2.3$ μm) at $\lambda = 0.813$ μm. Our results are also in good agreement (see Table 1) with the dispersion and the slope dispersion calculated by Brechet et al. for the same structure by a finite-element method.[17]

3. Results

In the examples given in what follows, we simulate a MOF made from a subset of triangular array of cylindrical air inclusions ($n_i = 1$) of lattice pitch Λ. The inclusions have identical circular cross sections of diameter d; the core is formed by a missing inclu-

Table 1. Comparison of Dispersion *D* and Its Slope Measured and Calculated at $\lambda = 0.813$ μm by Gander *et al.*[a]

Dispersion		Dispersion Slope	
Measured	Calculated	Measured	Calculated
-77.7^b	-77^b	0.464^a	
	-78.6^c		0.450^c
	-76.95 ($N_r = 4$)^d		0.455 ($N_r = 4$)^d
	-76.78 ($N_r = 3$)^d		0.458 ($N_r = 3$)^d

[a]They did not compute the dispersion slope, and the N_r value is not given in their text, so only an estimated value can be deduced from the scanning-electron micrograph of the MOF that they show as Fig. 2 of their paper[16]; the results by Brechet et al.[17] with a finite-element method at $\lambda = 0.813$ μm and the results with our multipole method for two values of N_r at the same wavelength are also shown here. Unit for dispersion, ps nm^{-1} km^{-1}; unit for the dispersion slope, ps nm^{-2} km^{-1}.
[b]Results of Gander et al.[16]
[c]Results of Brechet et al.[17]
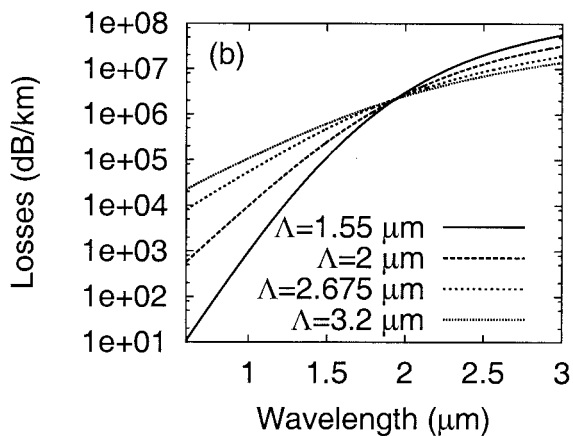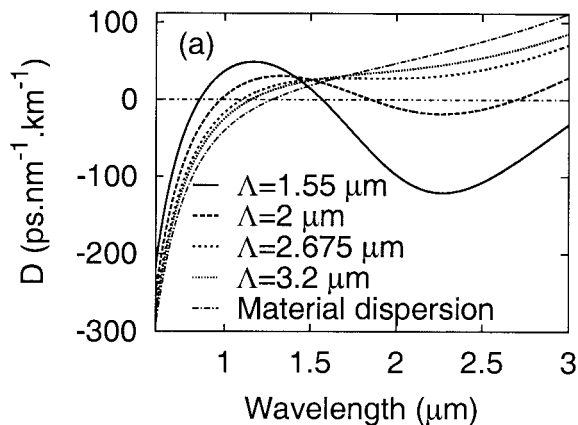[d]Results of our multipole method for two values of N_r.

Fig. 2. (a) Dispersion and (b) losses for a three-ring MOF as a function of wavelength and pitch Λ. The material dispersion is also shown. Hole diameter d, 0.8 μm.

Fig. 3. Losses for a four-ring MOF as a function of wavelength and pitch Λ. Hole diameter d, 0.8 μm. The y scale is linear, unlike for Fig. 2(b).

sion (see Fig. 1). The finite thickness of the hole region about the core can be described by the number of rings of holes N_r. The matrix and the jacket are made from silica, so the guiding structure is formed by a finite number of low-index inclusions in infinite silica bulk (the Sellmeier expansion is taken from Ref. 8). Because the hole region surrounding the core is bounded, it is clear that propagating modes are leaky.

We limit our study to the properties of fundamental mode dispersion, and the wavelengths that we consider here are included in the range 0.6–3 μm. As shown in Fig. 2 for a fixed hole diameter, a small pitch generates oscillations of the dispersion, and several zero-dispersion wavelengths can be found. With a larger pitch, the dispersion increases monotonically with wavelength. This property can be understood as follows: For large pitch, the MOF core is large too, the waveguide effects on dispersion are therefore weak; thus the material dispersion dominates. Conversely, for smaller pitches the waveguide dispersion takes over, and we observe oscillations of the dispersion curve; the amplitude of these oscillations increases as the pitch decreases. In the short-wavelength limit, material dispersion is so negative
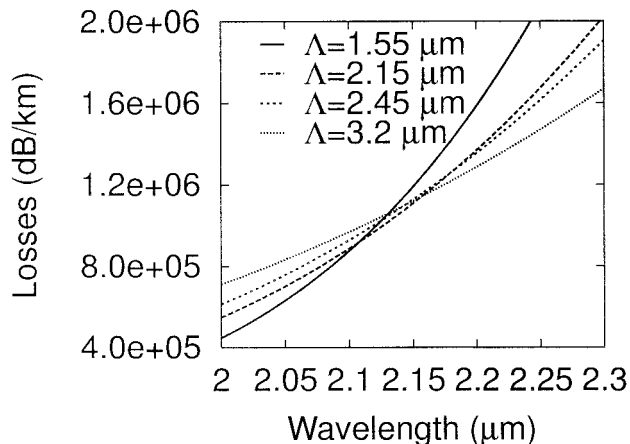
that waveguide dispersion cannot compensate for its effect. This remark explains why, for submicrometric wavelengths, all the dispersions tend toward material dispersion.

From Fig. 2 it can be noticed that there is a pitch value (Λ = 2.675 μm) for which the dispersion curve is flat over a large range of wavelengths when the average value is taken as 27.9 ps nm^{-1} km^{-1} near 1.85 μm, with the amplitude of dispersion oscillation equal to 0.2 ps nm^{-1} km^{-1} in a wavelength interval of 0.3 μm. For the same pitch but with $N_r = 4$ (data not shown) the dispersion curve is much less flat than with $N_r = 3$, and the average level of the dispersion has decreased; it is 23.7 ps nm^{-1} km^{-1} near 1.85 μm, with an amplitude of oscillation of 3.8 ps nm^{-1} km^{-1} in a wavelength interval of 0.5 μm. Notice that in both cases the corresponding losses (5.9 × 10^5 dB km^{-1} for $N_r = 3$ and 6.1 × 10^4 dB km^{-1} for $N_r = 4$) prohibit the use of these MOFs for practical applications. One can try to overcome this drawback by again increasing the number of rings, but this change entails a new change of the dispersion curve, as we show in detail in what follows. This example clearly shows the necessity for studying both losses and dispersion to achieve realistic dispersion engineering.

Another conclusion to draw from Fig. 2 is the existence of a wavelength, $\lambda_{cross} \simeq 1.93$ μm, for which the losses are almost independent of pitch Λ, at least in the range of Λ from 1.55 to 3.2 μm. This phenomenon occurs for other values of N_r: For $N_r = 4$, λ_{cross} is ~2.15 μm (see Fig. 3); for $N_r = 2$, λ_{cross} is ~1.63 μm (data not shown). The value of λ_{cross} increases slowly with N_r. A straight scale-law argument cannot be used because the hole's diameter is kept constant for the various structures. Besides, in as much as material dispersion depends on the actual wavelength, one must take care in using scaling arguments to try to explain this behavior. Material dispersion could also have an influence on the extent of the crossing region. Currently, the crossing region is approximately 0.1 μm large. From a math-
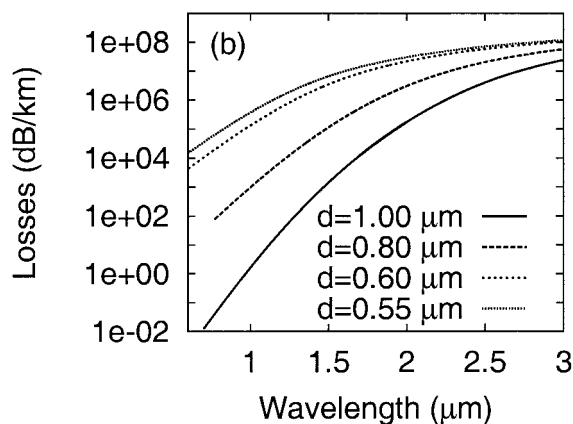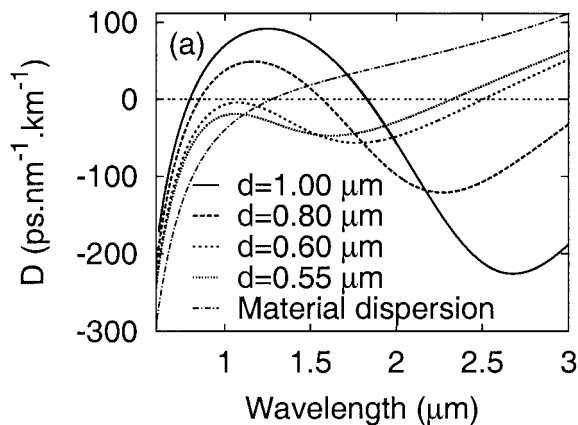
Fig. 4. (a) Dispersion and (b) losses for a three-ring MOF as a function of wavelength and hole diameter d. The material dispersion is also shown. Pitch Λ, 1.55 μm.
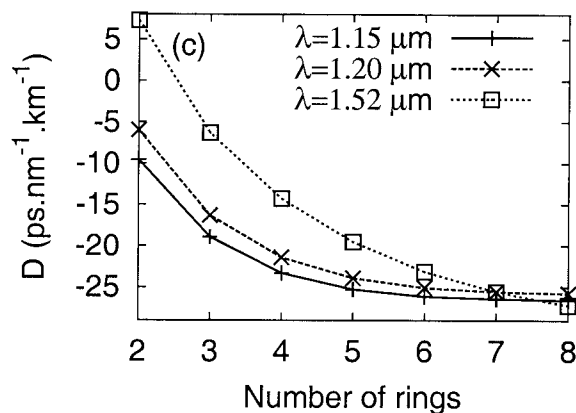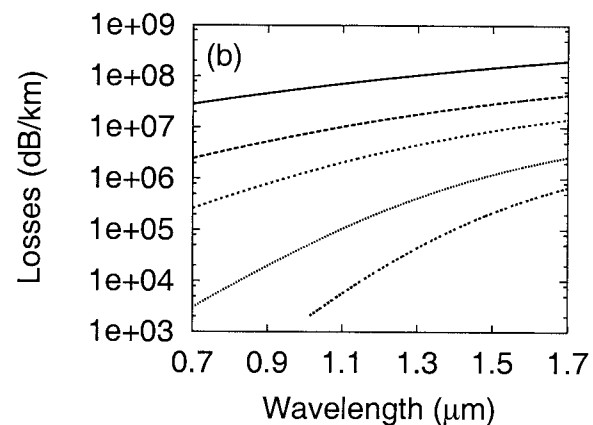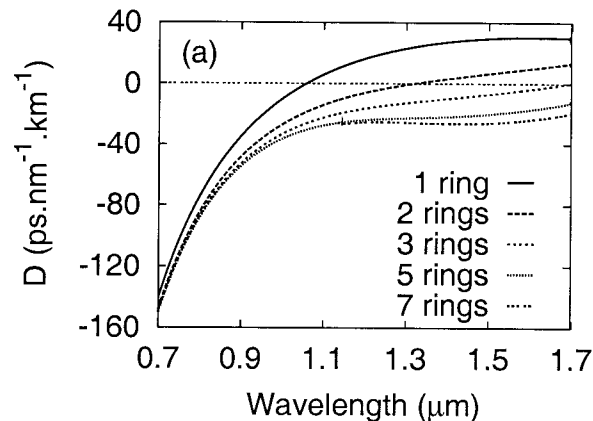

Fig. 5. (a) Dispersion and (b) losses as a function of the wavelength, and number of rings N_r [the types of curves have the same values for (a) and (b)]. Pitch Λ 2.0 μm; hole diameter d, 0.5 μm. (c) Dispersion for three wavelengths as a function of the number of rings N_r for the same MOF.

ematical point of view, for a fixed value of N_r the crossing phenomenon corresponds to point (λ_{cross}, Λ_{cross}) of surface $\mathscr{L}(\lambda, \Lambda)$ where the curve defined by $\partial\mathscr{L}/\partial\Lambda = 0$ crosses the curve given by $\partial^2\mathscr{L}/\partial\Lambda^2 = 0$. It seems more difficult to give the physical meaning of this phenomenon.

It can be seen from Fig. 4 that the oscillation amplitudes in dispersion curves increase with hole diameter (for $d = 1.00$ μm, i.e., d/Λ = 0.645, the oscillation amplitude (becomes 300 ps nm^{-1} km^{-1}). This behavior can be explained by consideration of MOF core size and by a competition between material dispersion and waveguide dispersion, similar to that given above for the influence of the pitch. It is worth noting that the value D_{max} of the dispersion's local maximum increases with hole diameter for all dispersion curves that we have computed. For three-ring MOFs with a fixed pitch $\Lambda = 1.55$ μm, the wavelength $\lambda_{D_{\text{max}}}$ associated with the local maximum D_{max} of dispersion increases with the diameter of the holes. One can use this property to shift the dispersion curves efficiently to obtain the required $\lambda_{D_{\text{max}}}$.

One can try to reduce the huge losses [more than 1.0×10^2 dB km^{-1} near $\lambda = 1.3$ μm for all the curves plotted in Fig. 4(a)] by increasing the number of hole

rings N_r, but once again dispersion profiles are modified. We now describe the influence of this crucial parameter. As shown in Fig. 5(a), when there is no local maximum of dispersion for MOFs with few rings, the dispersion decreases as the number of rings is increased. The difference between successive dispersion curves of two MOFs decreases as the number
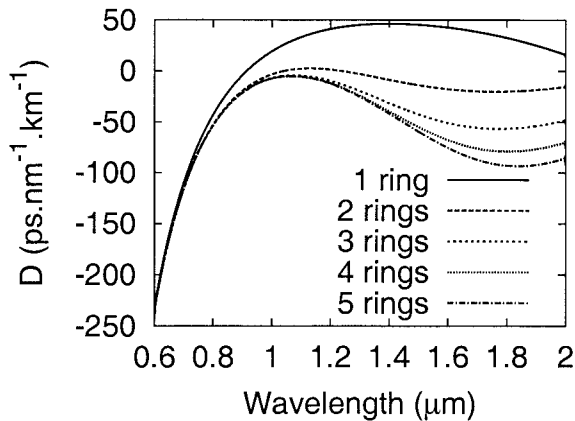
Fig. 6. Dispersion as a function of wavelength and number of rings N_r. Pitch Λ, 1.55 µm; hole diameter d, 0.6 µm.

of rings increases, as shown in Fig. 5(c). This figure clearly shows that the dispersion converges to a limit when the number of rings is increased. The convergence speed depends on the wavelength: The larger the wavelength, the slower the convergence [in Fig. 5(c) for $\lambda = 1.52$ µm the limit is not yet reached with eight rings]. It is worth noting that the losses associated with the flattened dispersion curve obtained with the seven-ring MOF of Fig. 5(a) are still large (more than 1.0×10^4 dB km^{-1} near $\lambda = 1.3$ µm). This influence of N_r on dispersion can be understood in the following way: When losses are weak, a supplementary ring will not change the mode drastically. In contrast, when the mode is not well confined in the core, a supplementary ring will modify the mode significantly. We can thus assume that the field pattern associated with the mode converges with increasing N_r; the convergence is slower for larger wavelengths because modes are less confined for these wavelengths. As opposed to the example in Fig. 5(a), for structures whose dispersion does exhibit oscillatory behavior [e.g., structures of small pitch in Fig. 2(a), which have a high diameter/pitch ratio], an increase of N_r results in amplification of the oscillation amplitude (see Fig. 6).

4. Conclusion and Discussion

As was shown in Section 3, one cannot keep the flattened dispersion with a fixed D value obtained for certain MOFs and at the same time reduce the MOFs' losses through a simple increase of their number of air-hole rings.

It must also be pointed out that an increase of the number of rings can reduce the losses of higher-order modes. As a consequence, a monomode fiber may become multimode for some configurations. Nevertheless, if large differences between the real parts of n_{eff} for the modes are found, mode coupling between the fundamental mode and the higher-order mode should be suppressed. We continue to study these effects and the influence of the jacket on dispersion.

The high loss figures that we have reported throughout this paper might give the wrong impression that low losses are not feasible in microstructured fibers, but low-loss MOFs are possible with appropriate geometric parameters[9] [see also the loss curve at small wavelengths for $d = 1.0$ µm in Fig. 4(b)]. For example, with $\Lambda = 2.26$ µm, d = 1.51 µm, and $N_r = 3$ the losses that we compute are below 1×10^{-4} dB km^{-1} at a wavelength of 0.76 µm. The same structure with $N_r = 7$ corresponds to that studied experimentally by Kubota and his colleagues.[18] The measured global losses at a wavelength of 0.85 µm are 7.1 dB km^{-1}, which clearly shows that the losses in MOFs can be limited by Rayleigh scattering, structural imperfections, and absorption and not by the geometrical losses. But interesting dispersion properties seem to imply geometrical parameters that are not necessarily compatible with low losses and few air-hole rings.

The issue for dispersion engineering applications is to find MOF parameters that produce both ultraflattened dispersion curves (negative, positive, or nearly zero) about the specified wavelength (for example, 1.3 or 1.55 µm) and low losses (near or below 1 dB km^{-1}). Consequently, for such engineering the finite size of the fiber cross section must be considered. Accurate design of such MOFs is currently under study.[19]

References and Notes

1. D. Mogilevstev, T. A. Birks, and P. St. J. Russell, "Group-velocity dispersion in photonic crystal fibers," Opt. Lett. **23,** 1662–1664 (1998).
2. J. C. Knight, J. Arriaga, T. A. Birks, A. Ortisaga-Blanch, W. J. Wadsworth, and P. St. J. Russell, "Anomalous dispersion in photonic crystal fibers," IEEE Photon. Technol. Lett. **12,** 807–809 (2000).
3. T. P. White, B. Kuhlmey, R. C. McPhedran, D. Maystre, G. Renversez, C. M. de Sterke, and L. C. Botten, "Multipole method for microstructured optical fibers. I. Formulation," J. Opt. Soc. Am. B **19,** 2322–2330 (2002).
4. B. Kuhlmey, T. P. White, G. Renversez, D. Maystre, L. C. Botten, C. M. de Sterke, and R. C. McPhedran, "Multipole method for microstructured optical fibers. II. Implementation and results," J. Opt. Soc. Am. B **19,** 2331–2340 (2002).
5. R. C. McPhedran and L. C. Botten, Department of Mathematical Sciences, University of Technology, Sydney, New South Wales 2007, Australia.
6. M. J. Steel, T. P. White, C. M. de Sterke, R. C. McPhedran, and L. C. Botten, "Symmetry and degeneracy in microstrutured optical fibers," Opt. Lett. **26,** 488–490 (2001).
7. J. W. Fleming, "Material dispersion in lightguide glasses," Electron. Lett. **14,** 326–328 (1978).
8. G. P. Agrawal, *Nonlinear Fiber Optics* (Academic, San Diego, Calif., 1989).
9. T. P. White, R. C. McPhedran, C. M. de Sterke, L. C. Botten, and M. J. Steel, "Confinement losses in microstructured optical fibers," Opt. Lett. **26,** 1660–1662 (2001).
10. A. Ferrando, E. Silvestre, J.-J. Miret, P. Andrés, and M. V. Andrés, "Vector description of higher-order modes in photonic crystal fibers," J. Opt. Soc. Am. A **17,** 1333–1340 (2000).
11. A. Ferrando, E. Silvestre, J.-J. Miret, and P. Andrés, "Nearly zero ultraflattened dispersion in photonic crystal fibers," Opt. Lett. **25,** 790–792 (2000).
12. F. Zolla and R. Petit, "Method of fictitious sources as applied

to the electromagnetic diffraction of a plane wave by a grating in conical mounts," J. Opt. Soc. Am. A **13,** 1087–1096 (1996).

13. D. Felbacq, G. Tayeb, and D. Maystre, "Scattering by a random set of parallel cylinders," J. Opt. Soc. Am. A **9,** 2526–2538 (1994).

14. E. Centeno and D. Felbacq, "Scattering by a random set of parallel cylinders," J. Opt. Soc. Am. A **17,** 320–327 (2000).

15. P. R. Mc Isaac, "Symmetry-induced modal characteristics of uniform waveguides. I. Summary of results," IEEE Trans. Microwave Theory Tech. **23,** 421–433 (1975).

16. M. J. Gander, R. McBride, J. C. D. Jones, D. Mogilevtsev, T. A. Birks, J. C. Knight, and P. St. J. Russell, "Experimental measurement of group velocity dispersion in photonic crystal fibre, Electron. Lett. **35,** 63–64 (1999).

17. F. Brechet, J. Marcou, D. Pagnoux, and P. Roy, "Complete analysis of the characteristics of propagation into photonic crystal fibers by the finite element method," Opt. Fiber Technol. **6,** 181–191 (2000).

18. H. Kubota, S. Suzuki, S. Kawanishi, M. Nakazawa, and M. Takana. "Low-loss, 2 km-long photonic crystal fiber with zero GVD in the near IR suitable for picosecond pulse propagation at 800 nm band," in *Conference on Lasers and Electro-Optics (CLEO),* Vol. 56 of OSP Trends in Optics and Photonics (Optical Society of America, Washington, D. C., 2001), pp. CPD3–1–CPD3–2.

19. G. Renversez, B. Kuhlmey, and R. C. McPhedran are preparing the following paper for publication, "Dispersion management with microstructured optical fibers: ultra-flattened chromatic dispersion with low losses."